PROCEEDINGS OF SPIE

SPIEDigitalLibrary.org/conference-proceedings-of-spie

Band structures of cylindrical AlN/GaN quantum dots with fully coupled piezoelectric models

Prabhakar, Sanjay, Melnik, Roderick

Sanjay Prabhakar, Roderick Melnik, "Band structures of cylindrical AlN/GaN quantum dots with fully coupled piezoelectric models," Proc. SPIE 7764, Nanoengineering: Fabrication, Properties, Optics, and Devices VII, 77640A (27 August 2010); doi: 10.1117/12.861071

SPIE.

Event: SPIE NanoScience + Engineering, 2010, San Diego, California, United States

Band structures of cylindrical AlN/GaN quantum dots with fully coupled piezoelectric models

Sanjay Prabhakar,[1] and Roderick Melnik[1,2]

[1]M[2]NeT Laboratory, Wilfrid Laurier University, Waterloo, ON, Canada, N2L 3C5
[2]BCAM, Bizkaia Technology Park, 48160 Derio, Spain

ABSTRACT

We study the coupled electro-mechanical effects in the band structure calculations of low dimensional semiconductor nanostructures (LDSNs) such as AlN/GaN quantum dots. Some effects in these systems are essentially nonlinear. Strain, piezoelectric effects, eigenvalues and wave functions of a quantum dot have been used as tuning parameters for the optical response of LDSNs in photonics, band gap engineering and other applications. However, with a few noticeable exceptions, the influence of piezoelectric effects in the electron wave functions in Quantum Dots (QDs) studied with fully coupled models has been largely neglected in the literature. In this paper, by using the fully coupled model of electroelasticity, we analyze the piezoelectric effects into the band structure of cylindrical quantum dots. Results are reported for III-V type semiconductors with a major focus given to AlN/GaN based QD systems.

1. INTRODUCTION

AlN/GaN quantum dots are wide band gap semiconductor materials which attracted significant attention due to their current and potential applications in optical, optoelectronic and electronic devices used in nano- and bionano- technological applications. Self-assembled QDs are grown by Stranski-Krastanov process are of special interest because of its potential applications in QDs lasers, light emitting diodes as qubits for quantum computation and other applications.[1,2] Strain is induced due to the lattice mismatch at the interfaces between two different types of semiconductors which can be used as a tuning parameter in tailoring the electronic and optical properties of single and multiple self assembled quantum dots.[3–7]

A subject that has not been studied in detail in the context of AlN/GaN quantum dots, however, is the question of piezoelectric effects in single quantum dots, studied with fully coupled models. This is the subject of the present investigation. Our approach is closely related to that of Refs. 2, 8 but differs in a sense that we include the piezo-electric effects and strains into the Hamiltonian and develop a numerical approach based on the finite element method,[9] whereas the authors of Ref. 8 only studied the piezoelectric effects and did not consider the influence of these effects into the Hamiltonian to find the eigenvalues and wave functions in quantum dots. In the mean time, the authors of Ref. 2 did not account for the piezo-electric effects into the Hamiltonian and their research mainly concerned with the development of a theory in cylindrical coordinate representation of multi-band Hamiltonians.

In this paper, we present a numerical analysis of the band structure of single AlN/GaN QDs under the influence of electroelasticity. By using the Finite Element Method (FEM), we study the effect of electroelasticity on the electronic properties of cylindrical AlN/GaN QDs. Effect of several parameters such as electromechanical fields, strain, the eigenvalues and wave functions of single dots have been reported. We now turn to a discussion of our model, followed by a brief description of our computation methodology.

2. MATHEMATICAL MODEL

Electromechanical balance equations for wurtzite (WZ) structures are axisymmetric. Therefore, the original 3D problem can be reduced to a 2D problem. The coupled equations of WZ structure in the presence of

Nanoengineering: Fabrication, Properties, Optics, and Devices VII, edited by Elizabeth A. Dobisz, Louay A. Eldada,
Proc. of SPIE Vol. 7764, 77640A · © 2010 SPIE · CCC code: 0277-786X/10/$18 · doi: 10.1117/12.861071

electromechanical effects in cylindrical coordinates can be written as[10]

$$\frac{\partial \sigma_{\rho\rho}}{\partial \rho} + \frac{\partial \sigma_{\rho z}}{\partial z} + \frac{\sigma_{\rho\rho} - \sigma_{\phi\phi}}{\rho} = 0 \tag{1}$$

$$\frac{\partial \sigma_{\rho z}}{\partial \rho} + \frac{\partial \sigma_{zz}}{\partial z} + \frac{1}{\rho}\sigma_{\rho z} = 0 \tag{2}$$

$$\frac{\partial D_{\rho}}{\partial \rho} + \frac{\partial D_{z}}{\partial z} + \frac{1}{\rho}D_{\rho} = 0. \tag{3}$$

The stress tensor components and the electric displacement vector components can be written as

$$\sigma_{\rho\rho} = C_{11}\varepsilon_{\rho\rho} + C_{12}\varepsilon_{\phi\phi} + C_{13}\varepsilon_{zz} + e_{31}\partial_z V, \tag{4}$$

$$\sigma_{\phi\phi} = C_{11}\varepsilon_{\phi\phi} + C_{12}\varepsilon_{\rho\rho} + C_{13}\varepsilon_{zz} + e_{31}\partial_z V, \tag{5}$$

$$\sigma_{\rho z} = 2C_{44}\varepsilon_{\rho z} + e_{15}\partial_{\rho} V, \tag{6}$$

$$\sigma_{zz} = C_{13}\varepsilon_{\rho\rho} + C_{13}\varepsilon_{\phi\phi} + C_{33}\varepsilon_{zz} + e_{33}\partial_z V, \tag{7}$$

$$D_{\rho} = 2e_{15}\varepsilon_{\rho z} - \epsilon_1 \partial_{\rho} V, \tag{8}$$

$$D_z = e_{31}\left(\varepsilon_{rr} + \varepsilon_{\phi\phi}\right) e_{33}\varepsilon_{zz} - \epsilon_3 \partial_z V + P_z^{sp}. \tag{9}$$

where C_{kl} is the elastic moduli constant, e_{ij} is the piezoelectric constant, ϵ_{in} is the permittivity, V is the piezoelectric potential and $E = -\frac{\partial V}{\partial z}$ is the built in piezoelectric field. The strain tensor components due to lattice mismatch in a semiconductor can be written as[8, 11]

$$\varepsilon_{\rho\rho} = \frac{\partial u_{\rho}}{\partial \rho} + \varepsilon_a^{\star},\ \varepsilon_{zz} = \frac{\partial u_z}{\partial z} + \varepsilon_c^{\star}, \tag{10}$$

$$\varepsilon_{\phi\phi} = \frac{u_{\rho}}{\rho} + \varepsilon_a^{\star},\ \varepsilon_{\rho z} = \frac{1}{2}\left(\frac{\partial u_{\rho}}{\partial z} + \frac{\partial u_z}{\partial \rho}\right). \tag{11}$$

Here $\varepsilon_a^{\star} = \frac{a_m - a_{QD}}{c_{QD}}$ and $\varepsilon_c^{\star} = \frac{a_m - a_{QD}}{c_{QD}}$ are the local intrinsic strains along a and c directions, respectively. Also, a_m, c_m and a_{QD}, c_{QD} are the lattice constants of the matrix and the QD, respectively.

We consider the motion of electrons confined along the z-direction due to piezo-electric effect. Our approach closely related to that of Ref. 12. Therefore, the total Hamiltonian for the conduction band can be written as

$$H = H_{xyz} + H_e^{\varepsilon}. \tag{12}$$

Here, H_e^{ε} is the strain dependent part of the kinetic energy of the electron. The remaining portion of the Hamiltonian can be written as,

$$H_{xyz} = P_x \frac{1}{m_e^{\perp}} P_x + P_y \frac{1}{m_e^{\perp}} P_y + P_z \frac{1}{m_e^{\parallel}} P_z + E_c(r_e) + eV(r_e), \tag{13}$$

where the kinetic momentum operator $\vec{P} = -i\hbar\nabla$.

The strain dependent part of the electron Hamiltonian in (12) can be written as

$$H_e^{\varepsilon} = a_c^{\parallel}(r)\varepsilon_{zz}(r) + a_c^{\perp}(r)\left[\varepsilon_{xx}(r) + \varepsilon_{yy}(r)\right], \tag{14}$$

where $a_c^{\parallel}$ and $a_c^{\perp}$ are the conduction band deformation potentials along the symmetric and perpendicular to the symmetric axis. In cylindrical coordinates, we can write $\varepsilon_{xx} + \varepsilon_{yy} = \frac{\partial u_{\rho}}{\partial \rho} + \frac{u_{\rho}}{\rho} + 2\varepsilon_a^{\star}$, and

$$\begin{aligned} H_{\rho,z}^{k} &= -\frac{\hbar^2}{2m_0}\left[\frac{1}{\rho}\frac{\partial}{\partial \rho}\frac{\rho}{m_e^{\perp}}\frac{\partial}{\partial \rho} + \frac{\partial}{\partial z}\frac{1}{m_e^{\parallel}}\frac{\partial}{\partial z} - \frac{1}{\rho^2}\frac{1}{m_e^{\perp}}\ell^2\right] \\ &\quad + E_c + eV + a_c^{\parallel}\varepsilon_{zz} + a_c^{\perp}\left(\frac{\partial u_{\rho}}{\partial \rho} + \frac{u_{\rho}}{r} + 2\varepsilon_a^{\star}\right). \end{aligned} \tag{15}$$

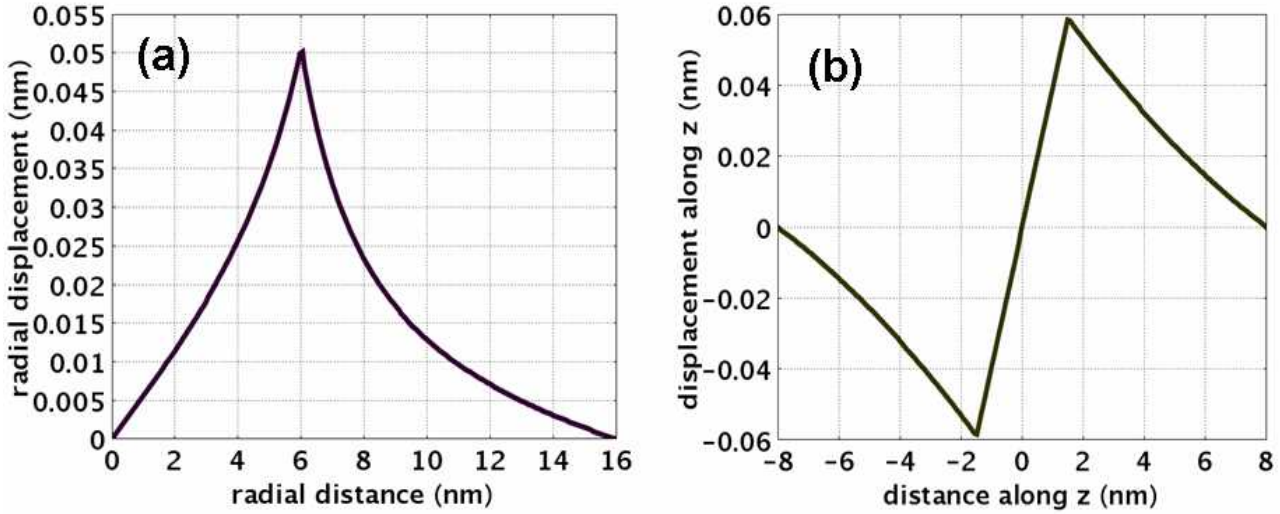

Figure 1. (a) Radial component of the displacement vs distance along ρ direction at z=0 and (b) displacement along z-direction vs distance along z-direction at $\rho = 0$

Six band hole Hamiltonian can be written in cylindrical coordinates as[2]

$$H^h_{\rho,z} = \begin{bmatrix} S_{11}+\triangle_1+\triangle_2 & S_{12} & S_{13} & 0 & 0 & 0 \\ S_{21} & S_{11}+\triangle_1-\triangle_2 & S_{23} & 0 & 0 & \sqrt{2}\triangle_3 \\ S_{31} & S_{32} & S_{33} & 0 & \sqrt{2}\triangle_3 & 0 \\ 0 & 0 & 0 & S_{44}+\triangle_1+\triangle_2 & S_{45} & S_{46} \\ 0 & 0 & \sqrt{2}\triangle_3 & S_{54} & S_{55}+\triangle_1-\triangle_2 & S_{56} \\ 0 & \sqrt{2}\triangle_3 & 0 & S_{64} & S_{65} & S_{66} \end{bmatrix}. \tag{16}$$

The details of the expressions for the symbols used in Eq. 18 are expressed in Ref. 2. Strain dependent part of the Hamiltonian can be written as

$$H^\varepsilon_h = \begin{bmatrix} h^\varepsilon_h & 0 \\ 0 & h^\varepsilon_h \end{bmatrix} + E_v + eV, \tag{17}$$

$$h^\varepsilon_h = \begin{bmatrix} l_1\varepsilon_{xx}+m_1\varepsilon_{yy}+m_2\varepsilon_{zz} & n_1\varepsilon_{xy} & n_2\varepsilon_{xz} \\ n_1\varepsilon_{xy} & m_1\varepsilon_{xx}+l_1\varepsilon_{yy}+m_2\varepsilon_{zz} & n_1\varepsilon_{xy} \\ n_2\varepsilon_{xz} & n_2\varepsilon_{yz} & m_3\left(\varepsilon_{xx}+\varepsilon_{yy}\right) \end{bmatrix}. \tag{18}$$

For a strained-layer wurtzite crystal pseudomorphically grown along c-direction, the strain tensor has only the following nonvanishing diagonal elements[13]

$$\varepsilon_{xx} = \varepsilon_{yy} = \frac{a_0 - a}{a}, \tag{19}$$

$$\varepsilon_{zz} = -\frac{2C_{13}}{C_{33}}\varepsilon_{xx}. \tag{20}$$

Finally, 8-band $k \cdot p$ Hamiltonian for wurtzite structure can be written as

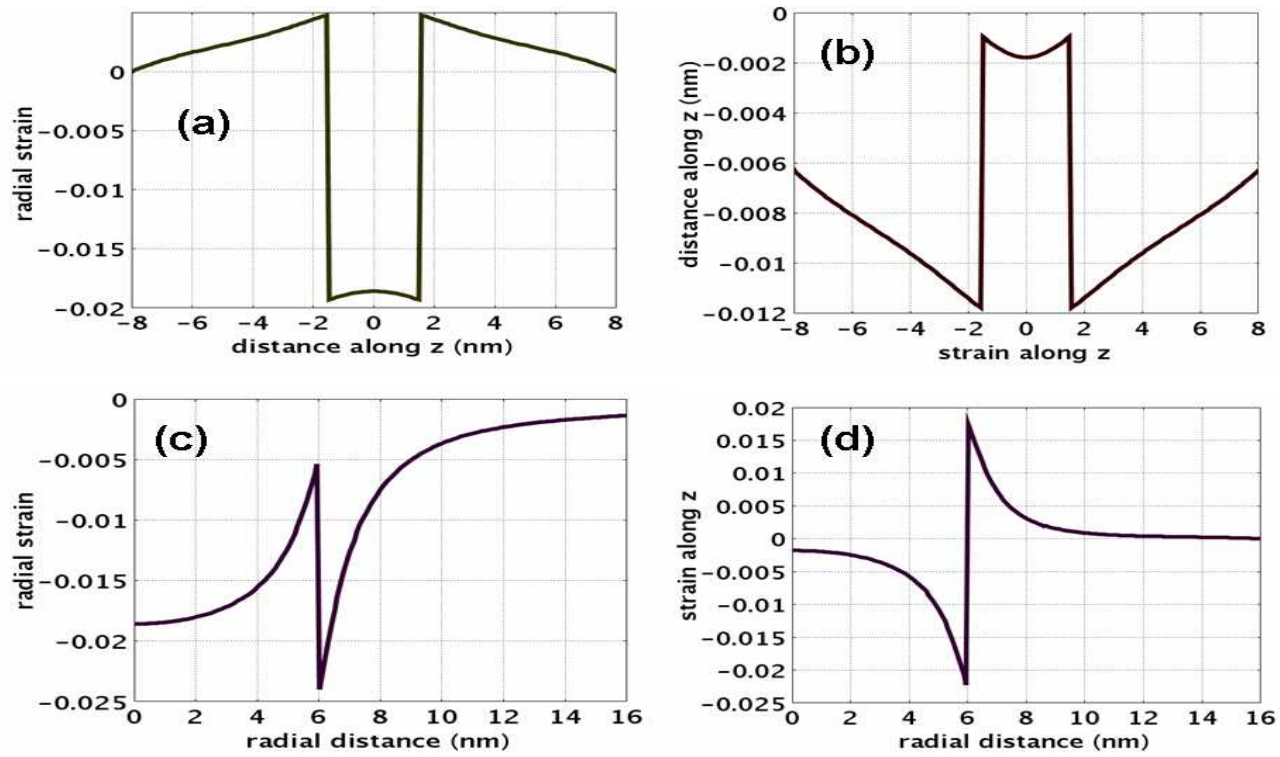

Figure 2. (a) Radial component of the strain vs distance along z-direction at $\rho = 0$ (b) z-component of the strain vs distance along z-direction at $\rho = 0$ (c) Radial component of the strain vs distance along ρ-direction at z=0 and (d) z-component of the strain vs distance along ρ-direction at z=0.

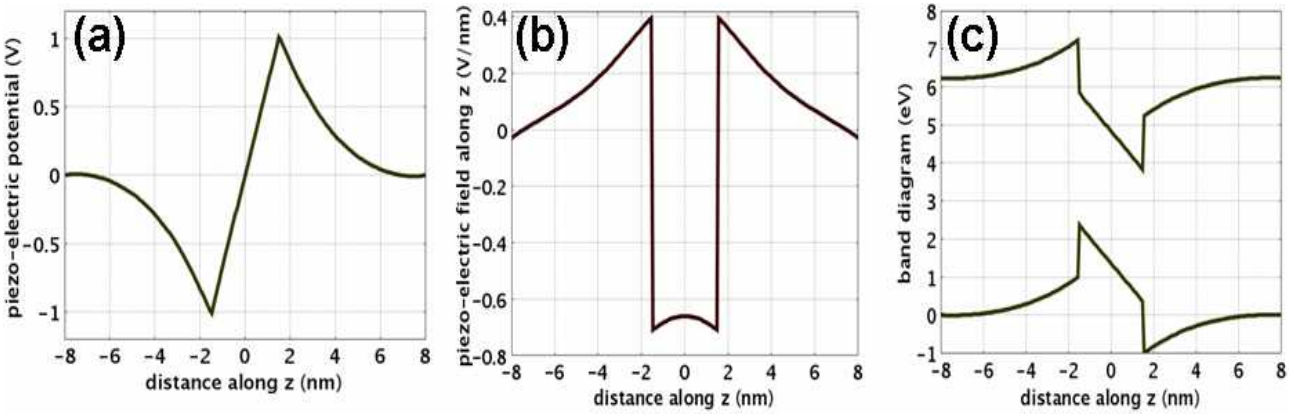

Figure 3. The influence of piezo-electric potential on the flat band diagram of AlN/GaN. (a) Piezo-electric field along z-direction at $\rho = 0$ and (b) effect of piezo-electric potential on the conduction and valence band of AlN/GaN quantum dot along z-direction at $\rho = 0$.

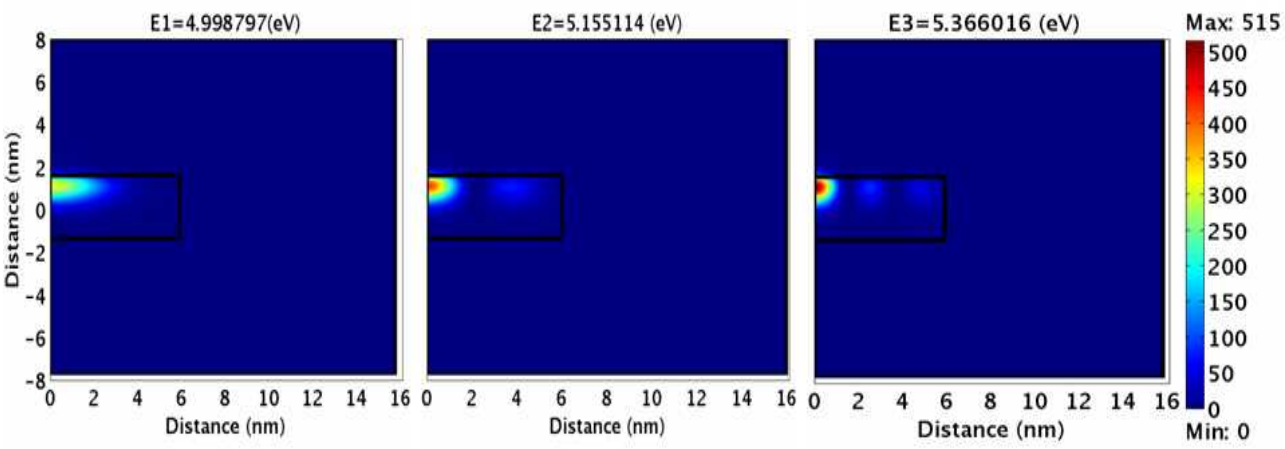

Figure 4. (Color online) The ground, first excited and second excited states eigenvalues and wave functions of the electrons in the conduction band of AlN/GaN quantum dot in the potential that has been considered in Fig 3(b). These eigenstates and eigenvalues have been found by solving 8-band $k \cdot p$ model.

$$H_{8\times 8} = \begin{bmatrix} H^k_{\rho,z} & & 0 & \\ & H^k_{\rho,z} & & \\ 0 & & H^h_{\rho,z} + H^\varepsilon_h & \end{bmatrix}. \tag{21}$$

We analyze the bandstructure of AlN/GaN material with an 8−band $k \cdot p$ model including piezo-electric effects based on Finite Element Method for different number of meshes and results are presented in the following section.

3. RESULTS AND DISCUSSIONS

The idea is to solve the coupled equation of 1 through 3 in cylindrical coordinates to get the realistic piezoelectric displacement, potential and strain. In the first step of our approach, we plotted the piezoelectric displacements along ρ and z-directions in cylindrical AlN/GaN quantum dots at $\rho = 0$ in Fig. 1(a) and $z = 0$ as in Fig. 1(b). Various components of the strain tensors have been plotted in Fig. 2. We plotted the piezoelectric potential, piezoelectric field and the effect of piezoelectric potential into the conduction and valence band diagram of AlN/GaN quantum dot along z-direction at $\rho = 0$ as shown in Fig. 3. Finally, we solve the 8−band $k \cdot p$ model in cylindrical coordinates to get the ground, first and second excited states eigenvalues and wave functions in a cylindrically shaped AlN/GaN quantum dot. These eigenvalues and wave functions are shown in Fig. 4. Note that the numerical convergence for these eigenvalues is achieved through the mesh refinements. For 11008 elements, the corresponding eigenvalues were 4.98805 eV, 5.155123 eV and 5.366032 eV.

4. CONCLUSIONS

We have carried out a numerical simulation study of electromechanical effects into eigenvalues and wave functions of AlN/GaN quantum dots. We accounted for the influence of piezoelectric effect on the band structure of single quantum dots based on a coupled numerical approach and the 8−band $k \cdot p$ method to obtain the eigenvalues and eigenstates.

The key result of this work is illustrated in Figs. 4: the spatial confinement of electron wave function is pushing towards z-direction in a cylindrical quantum dot and the eigenvalues of electrons are pushed further down due to strong built in piezo-electric potential along z-direction. We found that there is a strong built in piezo-electric potential in wurtzite structure at the interface which has a crucial impact in changing the localization of electron wave functions as well as eigenvalues into the conduction and valence band digram.

ACKNOWLEDGMENTS

This work was supported by NSERC and CRC program.

REFERENCES

1. S. J. Pearton, C. R. Abernathy, M. E. Overberg, G. T. Thaler, D. P. Norton, N. Theodoropoulou, A. F. Hebard, Y. D. Park, F. Ren, J. Kim, and L. A. Boatner, "Wide band gap ferromagnetic semiconductors and oxides," *Journal of Applied Physics* **93**(1), pp. 1–13, 2003.
2. L. C. L. Y. Voon, C. Galeriu, B. Lassen, M. Willatzen, and R. Melnik, "Electronic structure of wurtzite quantum dots with cylindrical symmetry," *Applied Physics Letters* **87**(4), p. 041906, 2005.
3. S. R. Patil and R. V. N. Melnik, "Coupled electromechanical effects in II − VI group finite length semiconductor nanowires," *Journal of Physics D: Applied Physics* **42**(14), p. 145113, 2009.
4. R. V. N. Melnik and R. Mahapatra, "Coupled effects in quantum dot nanostructures with nonlinear strain and bridging modelling scales," *Computers & Structures* **85**(11-14), pp. 698 – 711, 2007.
5. S. R. Patil and R. V. N. Melnik, "Thermoelectromechanical effects in quantum dots," *Nanotechnology* **20**(12), p. 125402, 2009.
6. R. V. N. Melnik and M. Willatzen, "Bandstructures of conical quantum dots with wetting layers," *Nanotechnology* **15**(1), p. 1, 2004.
7. R. V. N. Melnik and K. N. Zotsenko, "Finite element analysis of coupled electronic states in quantum dot nanostructures," *Modelling and Simulation in Materials Science and Engineering* **12**(3), p. 465, 2004.
8. D. Barettin, B. Lassen, and M. Willatzen, "Electromechanical fields in GaN/AlN wurtzite quantum dots," *Journal of Physics: Conference Series* **107**(1), p. 012001, 2008.
9. Comsol Multiphysics version 3.5a (www.comsol.com).
10. R. V. N. Melnik, "Generalised solutions, discrete models and energy estimates for a 2d problem of coupled field theory," *Applied Mathematics and Computation* **107**(1), pp. 27 – 55, 2000.
11. B. Lassen, M. Willatzen, D. Barettin, R. V. N. Melnik, and L. C. L. Y. Voon, "Electromechanical effects in electron structure for GaN/AlN quantum dots," *Journal of Physics: Conference Series* **107**(1), p. 012008.
12. V. A. Fonoberov and A. A. Balandin, "Excitonic properties of strained wurtzite and zinc-blende $GaN/Al_xGa_{1-x}N$ quantum dots," *Journal of Applied Physics* **94**(11), pp. 7178–7186, 2003.
13. S. L. Chuang and C. S. Chang, "k·p method for strained wurtzite semiconductors," *Phys. Rev. B* **54**, pp. 2491–2504, Jul 1996.